Intracellular acidification reduced gap junction coupling between immature rat neocortical pyramidal neurones

Birgit Rörig, Gaby Klausa and Bernd Sutor

Institute of Physiology, University of Munich, Pettenkoferstrasse 12, 80336 Munich, Germany

1. Developmental changes in electrophysiological properties of pyramidal neurones correlated with the developmental decline in gap junction-dependent dye coupling were investigated in coronal slices of rat prefrontal and sensorimotor cortex. Effects of intracellular acidification induced by application of weak organic acids on neuronal dye coupling, electrotonic parameters as well as synaptic potentials were examined using the patch clamp technique. Optical monitoring of intracellular pH revealed an acidic shift of 0·4–0·5 pH units following sodium propionate application.

2. Dye coupling between layer II–III neurones was prominent during the first two postnatal weeks. During this period, pre-incubation of slices with 30 mM of the sodium salts of weak organic acids reduced the number of cells coupled to the injected neurone by 64%.

3. Between postnatal days 1 and 18, the mean neuronal input resistance decreased significantly (by 81·0%). Both the membrane time constant (τ_0) and the first equalizing time constant (τ_1) also showed a significant developmental decline of 25·8 and 65·8%, respectively. Electrotonic length decreased by 34·9%. The electrophysiological properties of neurones displayed a pronounced intercellular variability which decreased with on-going development.

4. During the first two postnatal weeks, intracellular acidification led to a mean increase in neuronal input resistance of 55·9% and a mean decrease in electrotonic length of 22·2%. The membrane time constant was reduced by approximately 25% in the majority of neurones tested. Significant electrophysiological effects induced by intracellular acidification were not detected in uncoupled neurones from 18-day-old rats.

5. EPSP width at half-maximal amplitude showed a substantial reduction of approximately 50%, while rise times of the non-NMDA receptor-mediated EPSP components displayed no significant change during development. Both weak organic acids, as well as the gap junction blocker 1-octanol, reduced excitatory synaptic transmission independent of developmental age.

6. We conclude that gap junction permeability is regulated by intracellular pH in developing layer II–III pyramidal cells in the rat neocortex. The prominent correlation between pH-induced reduction in dye coupling and changes in electrophysiological cell properties suggests a significant influence of gap junctions on synaptic integration and information transfer in the immature neocortex.

In the developing rat neocortex, neuronal coupling via gap junctions has been observed between neuroblasts of the ventricular zone (Lo Turco & Kriegstein, 1991), embryonic cortical plate neurones (Mienville, Lange & Barker, 1994) and between pyramidal as well as non-pyramidal cells during the first postnatal weeks (Connors, Benardo & Prince, 1983; Peinado, Yuste & Katz, 1993). Dye-coupled cellular aggregates consist of column-like structures during the embryonic and the early postnatal period and smaller cell assemblies, so-called clusters, at later stages of development (Connors *et al.* 1983; Peinado *et al.* 1993; Mienville *et al.* 1994). The extent of dye coupling has been shown to decline drastically with development in rat (Connors *et al.* 1983; Peinado *et al.* 1993), ferret (Kandler, Douglas & Katz, 1994) and human neocortex (Cepeda, Walsh, Peacock, Buchwald & Levine, 1993).

The aggregation of large numbers of developing neurones into temporary syncytia suggests extensive metabolic and

electrical communication. However, up to now, the functional role of this extensive coupling in the immature neocortex remains speculative. Yuste, Peinado & Katz (1992) suggested a role for gap junctions in spontaneous coactivation of neuronal domains, which might represent a blueprint of the functional modules of the adult neocortex, i.e. the cortical columns. To date, the nature of the biochemical and/or electrical signals transmitted through these junctions is only incompletely understood. Gap junctions might mediate the exchange of second messengers or other growth signals between immature neurones. These signals might synchronize gene expression in a cluster or a column of coupled neurones. Clustered expression of the $GABA_A$ receptor α_1-subunit during development of rat cerebral cortex has been described recently (Paysan, Bolz, Mohler & Fritschy, 1994). Furthermore, the large number of junctions suggests strong influences on electrotonic cell properties, which might predominantly affect the dendritic tree where the majority of gap junctions as well as synaptic terminals are localized (Miller, 1988; Peinado *et al.* 1993).

In the developing ferret visual cortex, coupling via gap junctions has been considered to be a transitory communication system which disappears when synaptogenesis commences (Kandler *et al.* 1994). Although gap junctions and chemical synapses might gradually replace each other, there is a rather prolonged period of coexistence in rat neocortex, which coincides in part with the period of augmented plasticity during the second and third postnatal week (Perkins & Teyler, 1988). Morphological investigations demonstrate the presence of presumably excitatory synaptic terminals throughout the developing cortical plate by the time of birth (Miller, 1988) and spontaneous EPSPs as well as evoked EPSPs have been observed in rat anterior frontal cortex as early as postnatal day (P) 3 (Burgard & Hablitz, 1993). If gap junctions influence passive membrane properties, local regulation of gap junction permeability should alter the efficacy of synaptic potentials in the developing circuitry. Thus, gap junctions might crucially interfere with synapse stabilization and synaptic plasticity.

Up to now, the alterations in electrotonic cell properties induced by closure of gap junctions have not been directly demonstrated in neocortical pyramidal neurones during postnatal differentiation. We have therefore investigated to what extent uncoupling alters passive membrane parameters. The dependence of electrotonic neuronal properties on gap junction permeability would markedly influence the interaction between electrical and chemical synapses, especially during the period of circuit formation.

Possible physiological regulators of gap junctional conductance are changes in intracellular pH, an increase in intracellular Ca^{2+} and phosphorylation via different protein kinases (see Beyer, 1993, for review). Embryonic rat cortical neurones have been shown to uncouple after intracellular acidification (Lo Turco & Kriegstein, 1991; Mienville *et al.* 1994). However, the electrophysiological effects of intracellular pH changes have so far not been investigated during the postnatal period. In the present study, we investigated the effects of intracellular acidification induced by application of weak organic acids on electrotonic parameters in P4–P11 layer II–III pyramidal neurones. The low molecular weight tracer neurobiotin was used to demonstrate dye coupling and changes in dye coupling following intracellular acidification.

METHODS

Preparation of brain slices

Wistar rats of either sex, aged 1–18 days (the day of birth was designated as P0) were deeply anaesthetized with diethylether and decapitated. The brain was removed and stored for 1 min in physiological saline at 4 °C. Coronal slices (thickness, 500 μm) of prefrontal and sensorimotor cortex were prepared using a vibratome (Campden Instruments, London, UK). Slices were stored in artificial cerebrospinal fluid (ACSF) at room temperature (18–20 °C) for at least 1 h. Individual slices were transferred to a recording chamber and continuously perfused with ACSF at a flow rate of 4 ml min^{-1}. The ACSF contained (mM): 125 NaCl, 3 KCl, 2·5 $CaCl_2$, 1·5 $MgCl_2$, 1·25 NaH_2PO_4, 25 $NaHCO_3$ and 10 D-glucose. The osmolarity of the external solution was 306 mosmol l^{-1}. The solution was gassed continuously with carbogen (95% O_2–5% CO_2), resulting in a pH of 7·4 at a recording temperature of 31–32 °C. In the recording chamber, the slices were kept submerged by means of two nylon meshes, to aid mechanical stability. For intracellular acidification, 30 mM of the external NaCl was replaced by the sodium salts of either acetate, propionate or lactate. The external pH was kept at 7·3–7·4 by reducing the $NaHCO_3$ concentration to 15–18 mM. Changes in $NaHCO_3$ concentration were balanced by equimolar changes in NaCl.

Electrophysiological recording and stimulation

Blind whole-cell patch clamp recordings were performed as described previously (Blanton, Lo Turco & Kriegstein, 1989; Burghard & Hablitz, 1993). Patch pipettes were pulled from borosilicate tubing (Clark Electromedical Instruments, Reading, UK) and filled with a solution containing (mM): 125 potassium isethionic acid, 10 KCl, 0·5 EGTA, 10 Hepes and 2 MgATP. The pH was adjusted to 7·2 with NaOH. The osmolarity of the internal solution was 243 mosmol l^{-1} without, and 347 mosmol l^{-1} after the addition of neurobiotin (1 mg (100 μl)$^{-1}$). Tip resistances of the electrodes ranged between 4 and 6 MΩ when filled with normal internal solution. Recording pipettes were positioned in the superficial layers of the neocortex. A monopolar carbon-fibre stimulating electrode was placed at the white matter–layer VI border. Patch clamp recordings were obtained using a discontinuous single-electrode current and voltage clamp amplifier (NPI SEC-10L; Tamm, Germany) at a switching frequency of 26 kHz (duty cycle, 25%). Stimulus protocols for intracellular current injection were generated and neuronal responses were digitized using a Digidata 1200 analog-to-digital converter (Axon Instruments) in conjunction with pCLAMP software (Axon instruments). Signals were filtered at 3 kHz and stored on a computer for off-line analysis. Current clamp recordings were performed to determine resting membrane potential and input resistance (R_N). Input resistance was calculated from the membrane voltage response to a hyperpolarizing square-wave pulse (0·02 nA, 300 ms), which was monitored continuously on a

chart recorder (Dash IV; Astro Med, Rodgau, Germany). The membrane time constant (τ_0), first equalizing time constant (τ_1) and electrotonic length (L) were extracted from double exponential curves fitted to the initial phase of current pulse-induced voltage deflections using the AutesP program (H. Zucker, Garching Instruments, Munich, Germany). Action potentials were elicited by depolarizing square-wave current injections, 50–500 pA in amplitude and 35 ms duration. Developmental changes in amplitude, duration at half-maximal amplitude, rise time (10–90% amplitude) and fall time were investigated. Excitatory synaptic responses were evoked by application of 100–400 μA current stimuli of 50–100 μs duration. EPSP parameters analysed were 10–90% rise time and width at half-maximal amplitude. In most experiments, the non-NMDA component of the synaptic response was isolated by addition of 20 μM D-aminophosphonovalerate (APV). Recordings in slices from rats older than P7 were performed in the presence of 30 μM of the $GABA_B$ receptor antagonist CGP 35348 (Ciba-Geigy).

'Simulated' EPSPs were generated by injection of transient current pulses (amplitude, 100 pA; time to peak, 1 ms; decay time, 5 ms). Action potentials were recorded at a sampling frequency of 20 kHz; EPSPs and voltage responses to steady-state current injections at a sampling frequency of 4 kHz.

Statistical tests were performed using the program InStat (Graph Pad, San Diego, CA, USA). The significance of developmental changes in electrophysiological properties was evaluated by a non-parametric ordinary ANOVA. Differences in standard deviations were tested by Student's t test. The significance of changes in dye coupling following intracellular acidification was tested using the Mann–Whitney U test. Results are given as means ± S.E.M.

Determination of changes in intracellular pH

An optical recording technique was used to quantify the intracellular pH change induced by the application of weak organic acids (Buckler & Vaughan-Jones, 1990). Cells were loaded with the pH-sensitive fluoroprobe carboxy-seminaphthorhodafluor-1 (carboxy-SNARF-1; Molecular Probes) by incubation of the slices for at least 2 h in ACSF containing 10 μM of the acetoxymethyl ester of the pH-sensitive dye. To reduce photobleaching of the dye, the incubation of the slices was performed in the dark. Carboxy-SNARF-1-loaded slices were fixed in a recording chamber placed on the stage of an inverted microscope (IM35; Zeiss). Within an area of the neocortex of 0·1 mm^2, fluorescence was elicited by exciting the dye with light at a wavelength of 515 nm. The light was applied as pulses 100 ms in duration, at a frequency of 0·1 Hz for several minutes. The emitted fluorescence was divided into two beams using a dichroic mirror and recorded simultaneously at 580 and 640 nm by means of two photodiodes. The pH changes were calculated off-line from the signal ratios (580/640 nm).

Neurobiotin injections and histological processing

To study dye coupling as well as the morphology of developing pyramidal neurones, the low molecular weight tracer neurobiotin (Vector, Burlingame, CA, USA) was added to the recording pipette at a concentration of 1%. Following recordings, the slices were stored for 1 h in gassed saline at room temperature to allow the tracer to spread to neighbouring cells. The slices were then fixed for 1 h in 5% paraformaldehyde in 0·1 M phosphate-buffered saline (PBS) and stored overnight in 50% saccharose in PBS. To visualize tracer-filled neurones, slices were resectioned at 50 μm on a freeze-cut microtome (2055 Autocut; Leica Instruments, Benzheim, Germany). Sections were rinsed in PBS containing NaCl (0·1 M, pH 7·3, 3 × 10 min) and treated with Triton X-100 (0·5% (v/v) in PBS, 2 × 10 min). The sections were then incubated in avidin-conjugated horseradish peroxidase (HRP; 1% in PBS; Vector) for 90 min. Following rinses in PBS for 10 min and Tris–HCl (0·5 M, pH 8) for 2 × 10 min, the sections were pre-incubated in 0·5% diaminobenzidine (in Tris–HCl, pH 8) for 15 min. Hydrogen peroxide solution was added at a final concentration of 0·033%. The reaction was stopped by rinsing with Tris–HCl (2 × 10 min) and PBS (1 × 10 min). Sections were then mounted on glass slides, dehydrated in ethanol, cleared in xylene and coverslipped in Jung Tissue Freezing Medium (Leica Instruments).

Due to the relatively large tip diameter of patch pipettes (*ca* 1 μm), no ionophoretic ejection of the tracer was necessary. Mere diffusion resulted in clearly labelled neurones. To exclude staining of neurones produced by leakage of neurobiotin from the patch pipette into the extracellular space, control injections were performed in the following way. Patch pipettes were advanced into the tissue until the electrode resistance increased. Then the overpressure was removed and depolarizing current pulses of up to 0·5 nA were applied for a period of 10 min. In only one out of six trials was a small concentric dark spot found. Stained single neurones or neuronal aggregates were never observed following extracellular neurobiotin injection. Eighty-four out of eighty-nine filled neurones were recovered histologically. If the cell body or the dendrites of the patched neurone were damaged, the cell was excluded from analysis.

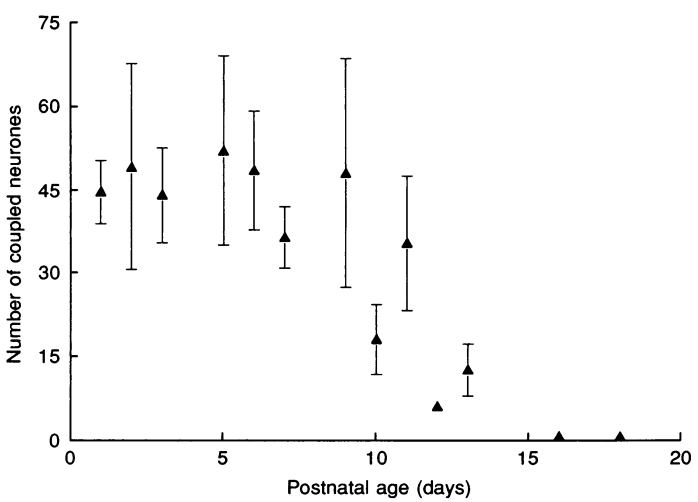

Figure 1. Reduction in dye coupling between layer II–III pyramidal cells during postnatal development

The mean number of cells (± S.E.M.) coupled to individual neurobiotin-filled neurones was plotted as a function of postnatal age. Dye coupling showed a considerable variability during the first two postnatal weeks and declined steeply after P13.

Tissue sections were photographed on a Nikon Biophot microscope. A Leitz NPL Fluotar ×40 objective lens and Nikon Plan ×20 and ×10 objective lenses were used for photography. Neurobiotin-stained neurones or neuronal clusters were reconstructed using a Leitz Laborlux microscope and a Leitz NPL Fluotar ×40 objective lens with a drawing tube attached to the microscope.

RESULTS

Developmental time course of dye coupling

Under normal conditions, the incidence of dye coupling (i.e. the number of labelled neurones displaying dye coupling in relation to the total number of filled cells) in frontal and sensorimotor cortex of the rat was 100% up to P12. Labelled neurones displaying no dye coupling did not appear before P13. The mean number of cells coupled to layer II–III pyramidal neurones was 46·4 ± 7·7 ($n = 7$) on P1 and P2. This number remained high during the first postnatal week, during which neuronal aggregates frequently occurred in a columnar shape (Fig. 4*A*). During the second postnatal week, the size of the cellular aggregates gradually declined (Fig. 1) and they tended to occur in concentric clusters rather than columns (Fig. 4*B*). On P18, the mean number of coupled cells per injection had decreased to 0·6 ± 0·4 ($n = 5$; Figs 1 and 4*C*). Within the first and second postnatal weeks, the number of neurones coupled to each other displayed a large variability that declined sharply after P13 (Fig. 1). To gain some insight into laminar differences in gap junction communication, eight layer V pyramidal neurones were filled with neurobiotin. On P7 and P8, the mean cluster size in lamina V was 22·4 ± 5·3 coupled cells per injection compared with a mean of 36·7 ± 4·4 ($n = 13$) in age-matched layer II–III neurones. Clusters containing less than ten neurones had

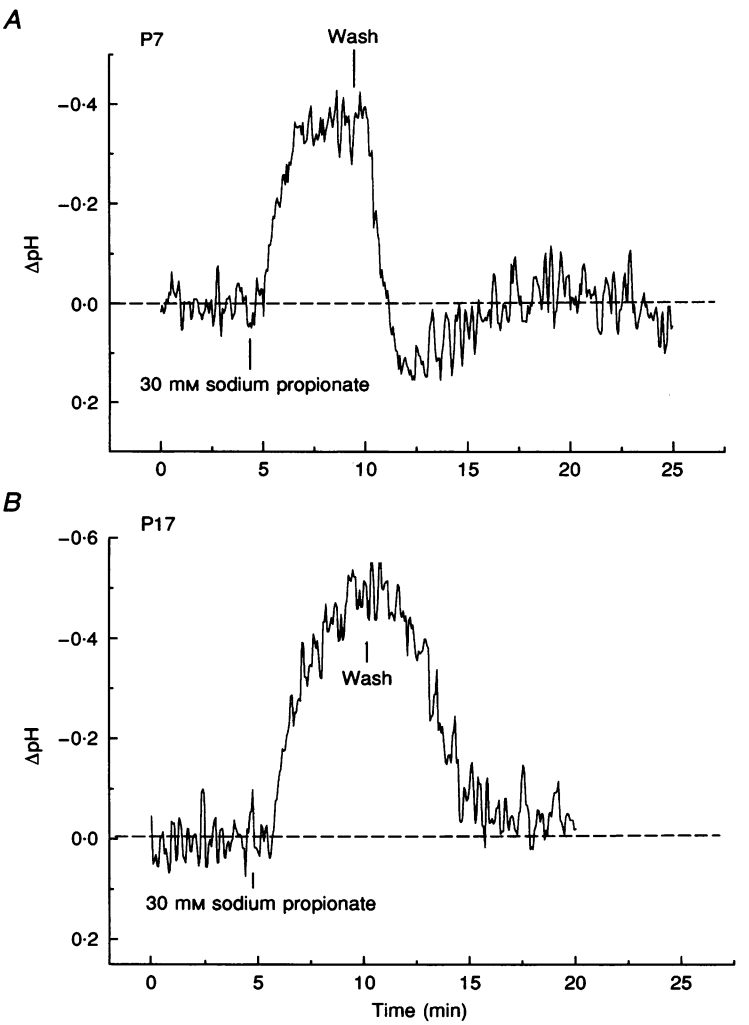

Figure 2. Time course of intracellular pH shifts induced by application of sodium propionate

Application of 30 mM sodium propionate on P7 induced an intracellular acidic shift of approximately 0·4 pH units within 1–2 min (*A*). Following washout of organic acids (Wash), a transient intracellular alkalosis of 0·18 pH units was observed. The time course of intracellular pH changes resembled the time course of alterations in input resistance produced by application of organic acids (see Fig. 8). In slices from P16–17 animals, acid application produced a decrease in intracellular pH of 0·5 pH units (*B*).

already appeared in layer V on P8 whereas such small clusters were not observed before P12 in the superficial layers. Thus, there seems to be a tendency for the developmental uncoupling process to start earlier in deeper layers.

Intracellular acidification induced by application of sodium propionate

Application of weak organic acids in order to achieve intracellular acidification in neurones of mammalian brain slice preparations has already been used (Perez-Velaquez, Valiante & Carlen, 1994). However, the magnitude of the intracellular pH shift has not been determined so far. We used the pH-sensitive fluoroprobe carboxy-SNARF-1 to estimate the acidic shift induced by application of 30 mM sodium propionate in four different cortical slices prepared from 7-day-old animals and in four slices from 16- to 17-day-old rats. The administration of sodium propionate (30 mM) to the ACSF produced an acidic pH shift followed by a transient alkalosis during washout of the compound (Fig. 2). The average acidification resulting from propionate treatment reached 0·37 ± 0·02 pH units on P7 (Fig. 2*A*). The average alkaline shift following washout of the organic acid was 0·185 ± 0·047 pH units ($n = 4$). On P16–P17 the average acidic shift was 0·51 ± 0·059 pH units ($n = 4$). An alkalosis following washout of organic acids was not observed in the older animals, which is probably due to the slower kinetics of recovery from the intracellular pH shift (Fig. 2*B*).

Reduction in dye coupling by intracellular acidification

To investigate the effect of intracellular acidification on gap junction coupling between developing pyramidal neurones, slices were incubated for at least 15–20 min in ACSF containing 30 mM of the sodium salts of either propionate, lactate or acetate. Whole-cell recordings were then performed, and cells filled with neurobiotin via diffusion from the patch pipette. Filling times and survival duration were standardized for acidified and control slices. Slices containing cells filled under conditions of lowered intracellular pH were stored in acid-containing solution for 1 h before fixation. During the first postnatal week (age group, P3–P6) the mean number of neurones dye coupled to the core cell was 41·4 ± 7·2 ($n = 8$) and the cluster size ranged between nineteen and seventy-four neurones (Fig. 3). After intracellular acidification, the mean cluster size was reduced by 62·6% to a mean value of 15·5 ± 2·9 coupled neurones per injection (range 4–37 cells, $n = 12$; Fig. 3). This effect was statistically significant ($P < 0·002$, Mann–Whitney U test). During the second postnatal week (P7–P11), the effects of intracellular acidification were identical (Fig. 3). The size of dye-coupled neuronal aggregates was reduced by 64·2% from a mean of 40·3 ± 5·7 coupled cells (range, 12–87 cells; $n = 13$) in control slices to a mean of 14·4 ± 2·8 coupled cells (range, 5–29 cells; $n = 9$) in slices treated with sodium propionate. This effect was also statistically significant ($P < 0·01$, Mann–Whitney U test). Examples of neurones filled under control conditions (*A–C*) and following intracellular acidification (*D* and *E*) are shown in Fig. 4. Figure 5 depicts camera lucida reconstructions of a control neurone (*A*), two cells filled in the presence of sodium propionate (*C* and *D*) and one cell filled during the application of ACSF containing sodium lactate (*B*).

Reduction in dye coupling by 1-octanol

In addition, we tested the effect of the well-known gap junction blocker 1-octanol on dye coupling between developing lamina II–III pyramidal cells on P7–P9. The mean number of coupled neurones under control conditions was 40·3 ± 5·9 (range, 17–85 cells; $n = 12$). Pre-incubation with 1-octanol (2 mM) significantly ($P < 0·0005$) reduced cluster size to a mean value of 12·85 ± 3·5 cells (range, 0–24 cells; $n = 13$; Fig. 3). Figure 4*F* shows a layer II pyramidal neurone completely uncoupled following incubation with 1-octanol.

Postnatal development of electrophysiological properties

In order to correlate developmental changes in dye coupling of neurones to alterations in their passive electrophysiological properties, action potentials and synaptic

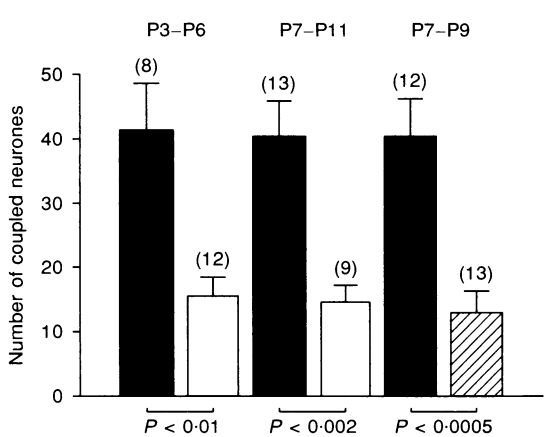

Figure 3. Reduction in dye coupling by intracellular acidification and 1-octanol

To compare dye coupling under control conditions and after intracellular acidification via 15–20 min incubation in 30 mM sodium propionate, neurones were split into two age groups (P3–P6 and P7–P11). Bars represent mean values of coupled cells per injection (± S.E.M.). The number of cells investigated is indicated in parentheses. ■, control; □, injection in the presence of sodium propionate (30 mM). The reduction in the mean number of coupled cells induced by intracellular acidification was statistically significant in both age groups (see text). On P7–P9, pre-incubation with 1-octanol (2 mM) also significantly reduced dye coupling (▨).

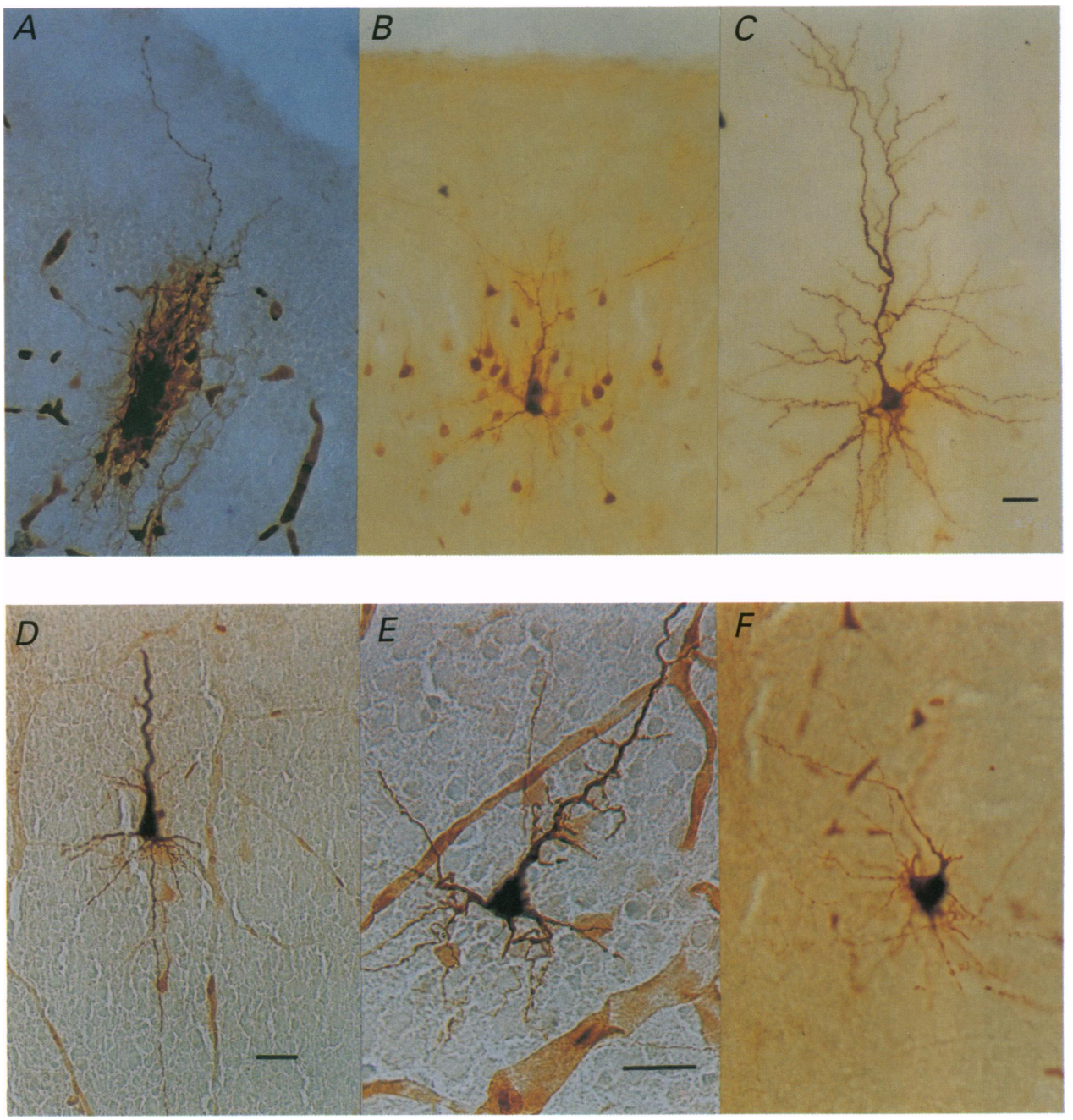

Figure 4. Developmental decline in dye coupling and uncoupling by pre-incubation in organic acids and 1-octanol

A–C, neurones filled under control conditions. On P1 (*A*), clusters of dye-coupled cells displayed a dense, columnar shape, whereas on P9 (*B*) labelled neurones were restricted to the core cell's dendritic tree. On P18 (*C*), dye coupling had completely disappeared in the majority of injected neurones. After pre-incubation in 30 mM sodium propionate (*D*), 30 mM sodium lactate (*E*) or 2 mM 1-octanol (*F*), the number of cells coupled to the injected neurone was drastically reduced even at developmental stages showing high coupling strength under control conditions (*D*, P4; *E*, P9; *F*, P8). Scale bars, 50 μm. Scale bar in *C* applies to *A* and *B*; scale bar in *E* applies to *F*.

potentials, the development of these parameters was investigated in layer II–III pyramidal cells from rats aged between P1 and P18. No subclassification of superficial layer pyramidal neurones was attempted.

Resting potential

The resting membrane potential was determined after a stable whole-cell recording had been established. The mean resting potential gradually increased during the first 3 weeks following birth from a mean of $-56{\cdot}3 \pm 1{\cdot}41$ mV ($n = 20$) on P1–P2 to $-70{\cdot}6 \pm 0{\cdot}95$ mV ($n = 19$) on P18. This developmental increase in resting membrane potential was statistically significant ($P < 0{\cdot}0001$, Kruskal–Wallis non-parametric ANOVA). The 25·4% increase in membrane potential was accompanied by a striking decrease in intercellular variability. The difference between standard deviations on P1–P2 and P18 was significant ($P < 0{\cdot}04$, unpaired t test).

Apparent input resistance

The input resistance was determined by injecting hyperpolarizing square-wave pulses (20 pA, 300 ms) at a frequency of 1 Hz through the patch pipette. The resulting voltage responses were digitized and averaged ($n = 10$). The apparent input resistance declined from a mean of $413{\cdot}1 \pm 29{\cdot}4$ MΩ ($n = 23$) on P1–P2 to a mean of

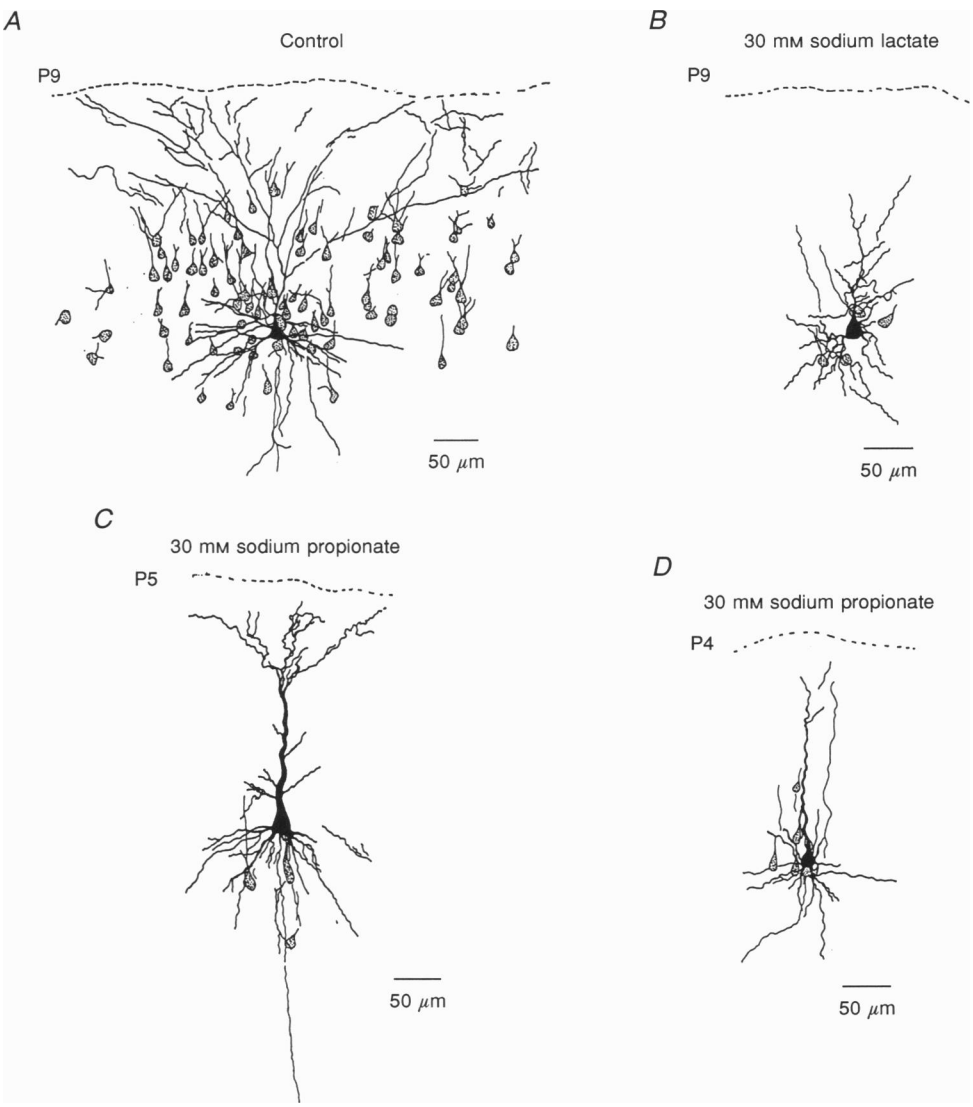

Figure 5. Camera lucida reconstructions of neurobiotin-filled cells

A, neurone filled under control conditions on P9; 82 coupled neurones were located in the vicinity of the core cell. *B*, in the presence of 30 mM sodium lactate, the number of dye-coupled cells was reduced to 4–5. *C* and *D*, examples of neurones (P4 and P5) filled after incubation in sodium propionate (30 mM). A drastic reduction in cluster size compared with control conditions (see Fig. 4) was observed.

83·9 ± 6·9 MΩ ($n = 22$) on P18 (Fig. 6). This developmental change in input resistance was statistically significant ($P < 0·0001$, non-parametric ANOVA). The developmental decrease in input resistance was associated with a marked reduction in its variability. The difference between standard deviations on P1–P2 and P18 was also significant ($P < 0·0001$, unpaired t test).

Membrane time constant and electrotonic length

The membrane time constant (τ_0), first equalizing time constant (τ_1) and electrotonic length were derived from double exponential curves fitted to the initial phase of voltage responses to square-wave hyperpolarizing current pulses. During the developmental period from P1–P2 to P18, the membrane time constant declined significantly ($P < 0·0012$, non-parametric ANOVA) from a mean of 17·27 ± 0·95 ms ($n = 20$) to a mean of 12·82 ± 0·92 ms ($n = 17$; Fig. 7*A*). Although a slight decrease in variability between individual neurones was observed with increasing age, the difference between standard deviations on P1–P2 and P18 was not statistically significant ($P < 0·329$, unpaired t test). The first equalizing time constant (Rall, 1969) also decreased from a mean of 3·13 ± 0·46 ms ($n = 9$) on P1 to a mean of 1·1 ± 0·2 ms on P18 ($n = 14$; Fig. 7*B*). The difference was statistically significant ($P < 0·0005$, non-parametric ANOVA). A strong decline in variability between individual neurones was observed (Fig. 7*B*); the difference between standard deviations on P1 and P18 was significant ($P < 0·09$, unpaired t test). The electrotonic length (L) was estimated according to the equation:

$$L = n\pi(\tau_0/\tau_1)^{½},$$

(Rall, 1969). The electrotonic length decreased significantly ($P < 0·0074$, non-parametric ANOVA) from a mean of 1·6 ± 0·1 ($n = 20$) on P1–P2 to a mean value of 1·1 ± 0·1 ($n = 17$; Fig. 7*C*) on P18. Again a decrease in variability was observed (Fig. 7*C*), and the difference between standard deviations on P1–P2 and P18 was significant ($P < 0·016$, unpaired t test).

Action potentials

Intracellular injection of suprathreshold depolarizing current pulses (duration, 35 ms) evoked single action potentials in all age groups tested. Trains of action potentials could be elicited as early as P1 by longer lasting depolarizing current pulses (300–500 ms). All recorded neurones were of the regular spiking type (Fig. 8*F*; see also Connors & Gutnick, 1990). Action potential amplitude (measured as peak amplitude with respect to resting membrane potential) did not change significantly during the period between P1 and P13. The mean values were 66·8 ± 3·65 mV on P1–P2 ($n = 9$) and 67·15 ± 2·2 mV ($n = 10$) on P11–P13. Action potential rise times decreased significantly ($P < 0·02$, non-parametric ANOVA) from a mean value of 0·89 ± 0·07 ms ($n = 10$) on P1–P3 to a mean of 0·57 ± 0·04 ms ($n = 11$; Fig. 8*B*) on P11–P13. Action potential fall times also declined significantly ($P < 0·002$, non-parametric ANOVA) from a mean of 5·76 ± 0·61 ms ($n = 10$) on P1–P3 to a mean of 1·99 ± 0·13 ms ($n = 11$; Fig. 8*C*) on P11–P13. Variability between individual neurones declined with increasing age (Fig. 8*B* and *C*). The standard deviations of fall times were significantly different between P1–P3 and P11–P13 ($P < 0·0001$, unpaired t test). Action potential width measured at half-maximal amplitude decreased significantly ($P < 0·001$, non-parametric ANOVA) from a mean of 3·65 ± 0·36 ms ($n = 12$) on P1–P3 to a mean of 1·61 ± 0·11 ms ($n = 11$) on P11–P13 (Fig. 8*A*). Intercellular variability also declined (Fig. 8*A*); the difference between standard deviations was statistically significant ($P < 0·0002$, unpaired t test). The change in action potential shape is illustrated in Fig. 8*D* and *E*.

As reported for layer V pyramidal cells (McCormick & Prince, 1987; Kasper, Larkman, Lübke & Blakemore, 1994), action potential rise times, fall times and duration at half-maximal amplitude also declined during postnatal development of lamina II–III neurones. These changes are probably due to an increase in ion channel density (Courand, Martin-Moutot, Koulakoff & Berwald-Neffer,

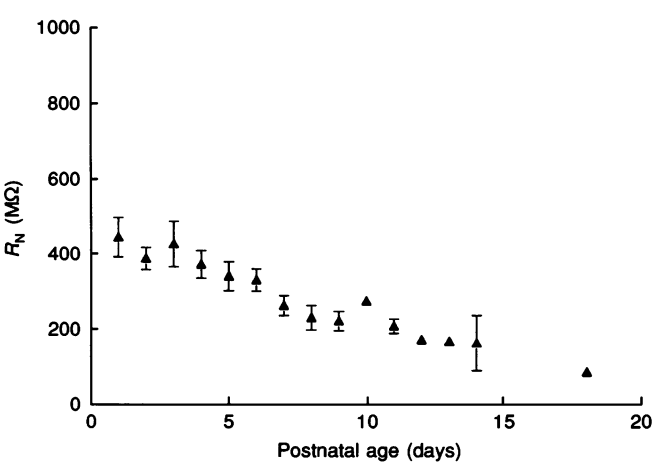

Figure 6. Age-related changes in neuronal input resistance

Mean values of input resistance (R_N; ± S.E.M.) of individual cells were plotted as a function of postnatal age. Input resistance declined significantly between P1 and P18. The variability among individual neurones decreased substantially during postnatal maturation of supragranular layer pyramidal cells.

1986). However, developmental changes in electrotonic parameters such as shortening of membrane time constants may also contribute to this phenomenon.

Effects of intracellular acidification on electrotonic cell properties

As revealed by filling of single neurones with neurobiotin, the size of dye-coupled neuronal clusters displayed a large variability during the first two postnatal weeks (Fig. 1). The variability of the number of coupled neurones, as well as the mean cluster size, gradually declined during the second postnatal week and dye coupling disappeared during the third week after birth (Fig. 1). This developmental time course of dye coupling was paralleled by a striking decrease in variability in the majority of the electrophysiological properties tested. The degree of gap junction coupling to neighbouring neurones might represent an important parameter shaping the apparent electrotonic membrane properties of an individual cell. We therefore intended to investigate to what extent uncoupling alters electrotonic parameters. Intracellular acidification significantly reduced dye coupling between layer II–III pyramidal cells (see above), thus demonstrating that gap junctions between developing neocortical pyramidal neurones are sensitive to changes in intracellular pH. In order to investigate the electrophysiological effects of lowering intracellular pH, neurones were patched in control ACSF, and 30 mM of either sodium propionate or sodium acetate were added to the ACSF during the recording. Changes in input resistance, membrane time constant and electrotonic length were analysed. Under control conditions, neuronal input resistance of P4–P13 pyramidal neurones ranged between 100 and 323 MΩ. In sixteen out of eighteen cells, application of 30 mM sodium propionate or sodium acetate induced a significant increase in input resistance (Fig. 9*A* and *C*) ranging between 21·8 and 302·4% (55·9 ± 18·3%). Under control conditions, the electrotonic length of P4–P13 neurones varied between 1·004 and 1·737. In fourteen out of eighteen neurones tested, lowering the intracellular pH induced a decrease in

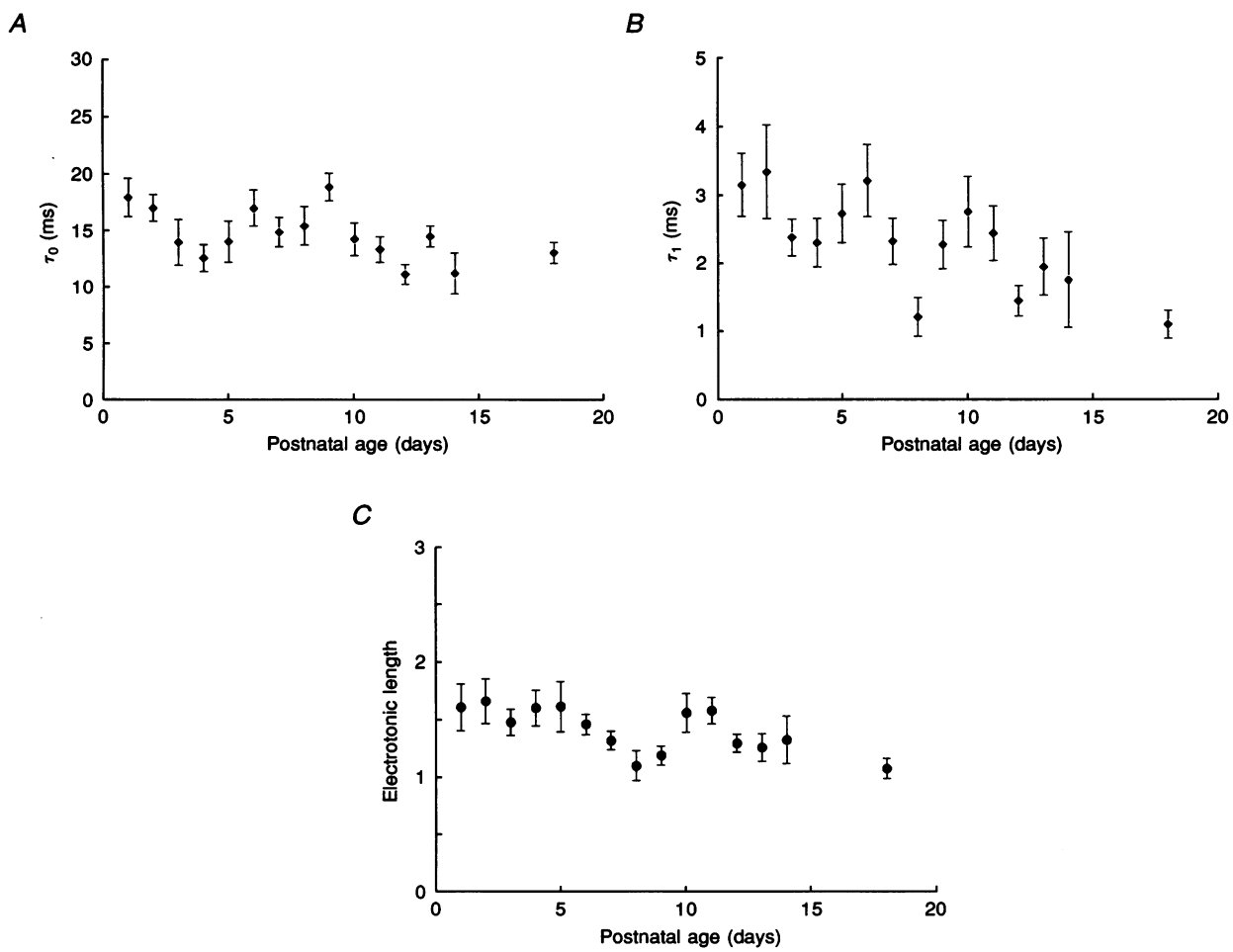

Figure 7. Postnatal maturation of subthreshold membrane properties

Diagrams show mean values (± S.E.M.) of membrane time constant (τ_0; *A*), first equalizing time constant (τ_1; *B*) and electrotonic length (*C*) as a function of postnatal age. Note that, for all parameters investigated, the variability between individual neurones declined.

electrotonic length ranging between 5·1 and 49·8% (22·2 ± 3·7%). This alteration in electrotonic length was probably due to a more pronounced decrease in the first equalizing time constant τ_1 (88·4 ± 53·42%; $n = 14$) compared with the changes in the membrane time constant τ_0 (24·3 ± 5·19%; $n = 10$). In two out of sixteen neurones, the first equalizing time constant increased slightly (6 and 12%) and in six out of sixteen neurones investigated, the membrane time constant was found to be enhanced by about 50%. Following washout of the organic acids, a decrease in input resistance beyond control conditions was frequently observed (Fig. 9*A* and *C*). The transient reduction in input resistance might be caused by the transient intracellular alkalosis following diffusion of the protonated acid molecule across the cell membrane. The time course of changes in input resistance during and after application of organic acids is shown in Fig. 9*E* and *F*.

In order to verify that the observed effects of intracellular acidification were due to gap junction blockade, the effects of weak organic acids on electrotonic membrane properties were also investigated in P18 neurones. At this age, filling of cells with neurobiotin resulted in staining of either a single neurone or only one to two coupled cells. (Figs 1 and 4). On P18, input resistance was found to be unaffected following application of sodium propionate or sodium acetate in six out of eleven neurones tested (Fig. 9*B* and *D*). In the remaining five cells, a small mean increase of 6·6 ± 2·77% was observed. Electrotonic length and membrane time constants were virtually unaltered in all neurones tested ($n = 11$). Although application of weak

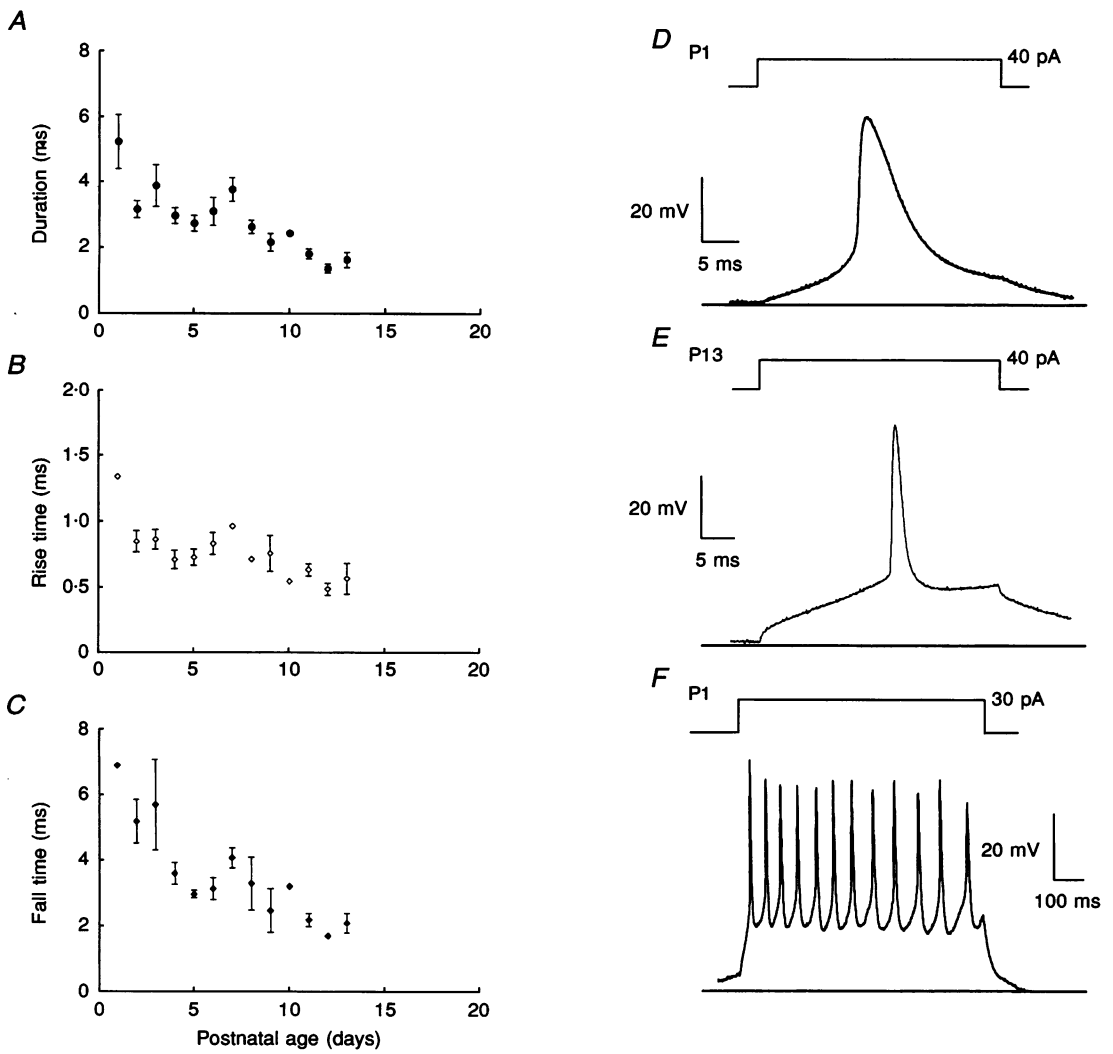

Figure 8. Age-related changes in action potentials

Mean values (± S.E.M.) of action potential duration measured at half-maximal amplitude, action potential rise time and action potential fall time are plotted as a function of postnatal age in *A*, *B* and *C*, respectively. Again, the considerable decline in variability between individual neurones is evident. Action potential width, rise time and fall time decreased significantly during postnatal development. Specimen recordings in *D* and *E* demonstrate that action potentials became both shorter and faster with on-going development. *F* illustrates the firing pattern of a P1 lamina III pyramidal cell.

organic acids still induced an intracellular pH shift of comparable magnitude (Fig. 2), the electrophysiological effects of intracellular acidification were no longer observed at developmental stages with a low incidence of dye coupling, suggesting that changes in electrotonic cell properties induced by intracellular acidification during the first and second postnatal week are indeed due to gap junction closure.

Synaptic potentials

The electrotonic structure of a neurone influences the efficacy of excitatory and inhibitory synaptic potentials. Regulation of electrotonic cell properties via modulation of gap junction permeability should thus affect chemical synaptic transmission in the developing neocortex. To investigate whether developmental uncoupling is paralleled by changes in EPSP kinetics, we analysed 10–90% rise times, as well as EPSP width measured at half-maximal amplitude, in neurones between P1 and P18. Since a significant alteration in EPSP kinetics due to a decreasing contribution of NMDA receptors during postnatal development has been reported (Burgard & Hablitz, 1993), we studied developmental changes of the isolated non-NMDA receptor-mediated EPSP. Recordings were therefore performed in the presence of 20 μM APV. The remaining non-NMDA receptor-mediated component was completely suppressed by 10 μM 6-cyano-7-nitroquinoxaline-2,3-dione (CNQX) in all neurones tested ($n = 4$). To avoid significant activation of inhibitory interneurones, near-threshold stimulus current intensities (50–400 μA) were used to elicit EPSPs. Furthermore, the membrane potential was held close to the theoretical Cl^- equilibrium potential (−67 mV) by current injection through the patch pipette. $GABA_B$ receptor-mediated late IPSPs were first observed

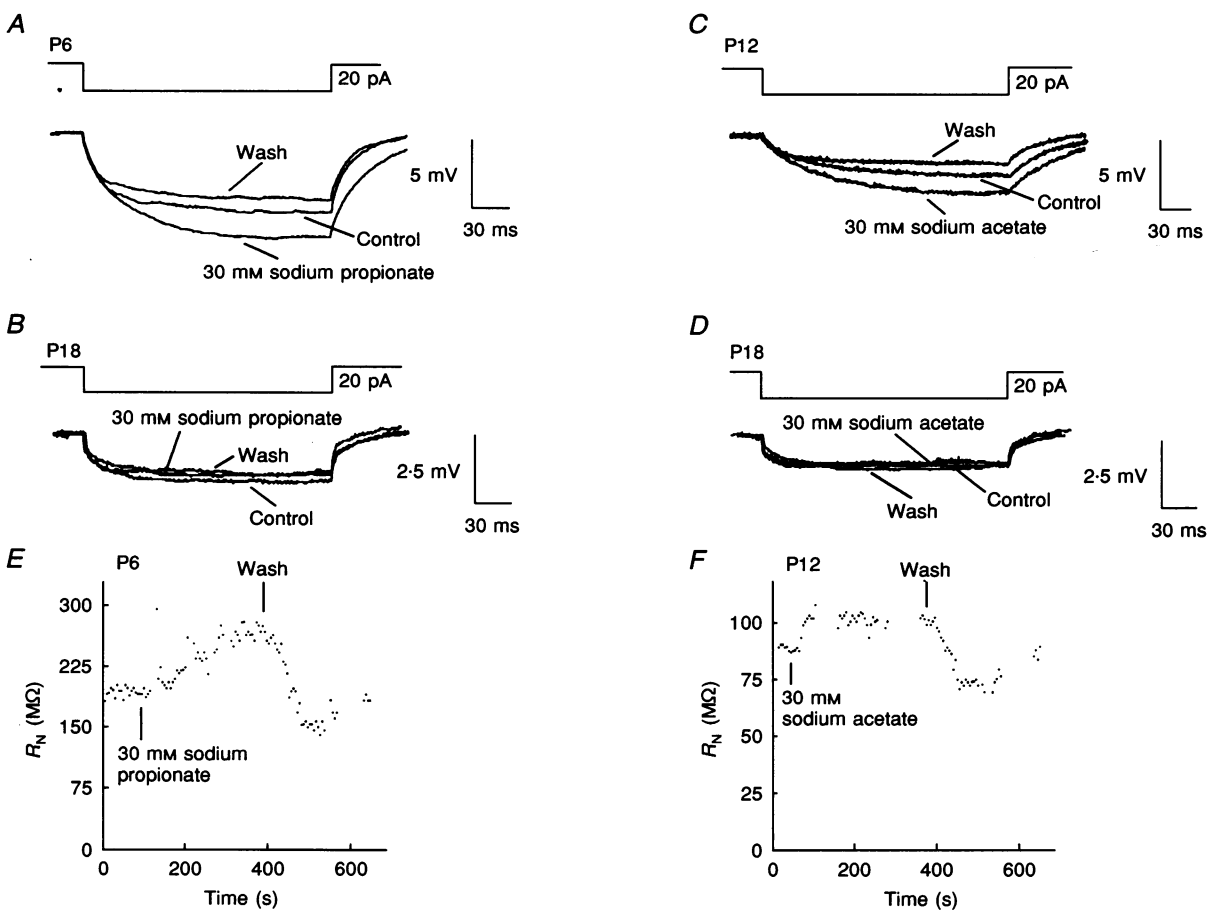

Figure 9. Effects of intracellular acidification on input resistance

During the first two postnatal weeks, application of 30 mM sodium propionate (*A*) or sodium acetate (*C*) caused a reversible increase in input resistance. The current pulse-induced voltage responses obtained before (Control), during and after (Wash) application of the compounds are superimposed. Note the reversible increase in decay time, indicating a prolongation of the membrane time constant in both examples. Recordings were performed at resting membrane potential. *B* and *D*, input resistance was virtually unaffected by intracellular acidification in neurones on P18. *E* and *F*, time course of changes in input resistance (R_N) following application and washout of organic acids. Input resistance transiently decreased beyond control levels after removal of the acid-containing solution suggesting that gap junctional conductance increases during the transient intracellular alkalosis.

on P7. Recordings during the second and third postnatal week were therefore performed in the presence of 30 μM of the $GABA_B$ receptor antagonist CGP 35348. Depolarizing postsynaptic potentials were elicited as early as P1. Stimulating electrodes were always placed at the white matter–layer VI border in an orthogonal position and at an equal distance from the recorded neurone to allow comparison between individual cells. For analysis, fifteen subsequently evoked single EPSPs were averaged. EPSP amplitudes ranged between 2·9 and 10·6 mV (Fig. 10*C* and *D*). The EPSP rise time did not change significantly between P1–P4 and P18 ($P = 0{\cdot}4154$, non-parametric ANOVA). On P1–P4, the mean value was $3{\cdot}76 \pm 0{\cdot}39$ ms ($n = 10$) and the mean value on P18 was $3{\cdot}77 \pm 0{\cdot}48$ ms ($n = 11$; Fig. 10*A*). In contrast, the EPSP duration measured at half-maximal amplitude declined significantly during postnatal development ($P = 0{\cdot}0457$, non-parametric ANOVA) from a mean value of $40{\cdot}84 \pm 5{\cdot}37$ ms ($n = 11$) on P1–P5 to a mean value of $22{\cdot}06 \pm 1{\cdot}91$ ms ($n = 12$) on P18 (Fig. 10*B*). Furthermore, the variability among individual neurones also declined (Fig. 10*A* and *B*); the difference between standard deviations on P1–P5 and P18 was statistically significant ($P < 0{\cdot}002$, unpaired t test). The developmental change in EPSP duration was still significant when the values were normalized with respect to the membrane time constants of the individual neurones ($P < 0{\cdot}02$, Mann–Whitney U test), indicating that the developmental shortening of membrane time constants is not the only factor responsible for the change in EPSP kinetics.

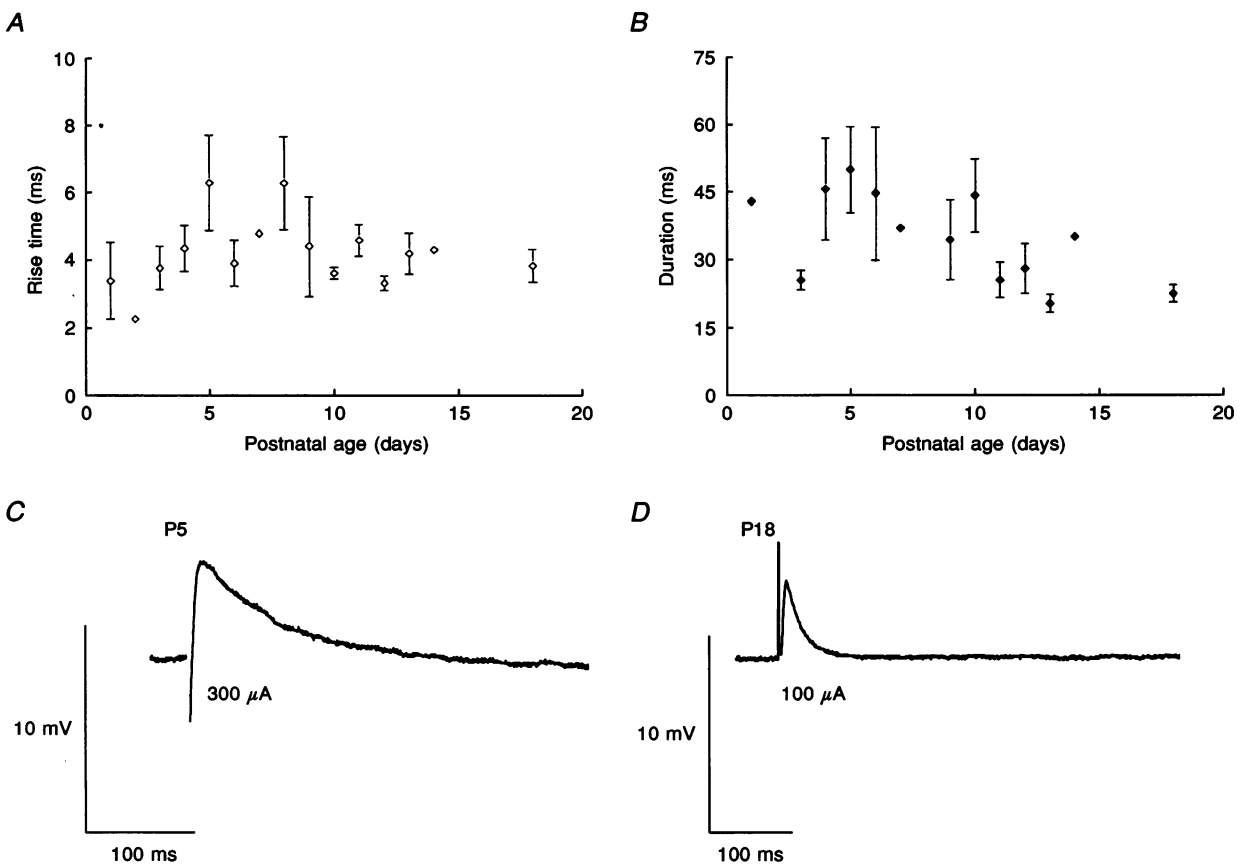

Figure 10. Developmental changes in shape parameters of non-NMDA receptor-mediated EPSPs

A and *B*, mean values (± S.E.M.) of the 10–90% rise time and EPSP duration measured at half-maximal amplitude, respectively, were plotted as a function of postnatal age. Rise times did not change significantly during postnatal maturation, whereas EPSP duration declined significantly. While the variability of rise times between individual neurones did not change significantly during postnatal development, the variability of EPSP durations declined at the end of the second postnatal week. *C* and *D*, specimen records demonstrating the developmental changes in EPSP waveform. *C*, EPSP recorded in a P5 layer II–III neurone. Stimulus strength, 300 μA for 100 μs; membrane potential (V_m) = −66 mV. *D*, EPSP recorded in a layer II–III neurone on P18. Stimulus strength 100 μA for 100 μs; $V_m = 71$ mV. Note the longer duration of the EPSP recorded in the younger neurone. All recordings were performed in the presence of 20 μM APV.

Effects of weak organic acids on EPSPs

Inhibition of dye coupling induced by a decrease in intracellular pH was associated with a considerable increase in input resistance and a decrease in electrotonic length (see above). Thus, excitatory synaptic potentials were expected to gain in efficacy following intracellular acidification. However, application of 30 mM sodium propionate reduced the amplitudes of EPSPs in six out of seven neurones tested (by 55·6 ± 14·4%; $n = 6$; Fig. 11). The inhibitory effect was variable, ranging from a 21% reduction in EPSP amplitude to a complete block (Fig. 11*A*). The depressant effect of acid application on EPSPs might be due to a direct influence of acidification or of organic acids, respectively, on either presynaptic calcium channels, transmitter release apparatus and/or postsynaptic receptors. However, the decrease in EPSP amplitude might also be explained by electrotonic uncoupling, given that part of the synaptic potential recorded under control conditions originated in neighbouring cells. In order to distinguish between these two possible explanations, the effects of organic acids on synaptic potentials recorded in P18 neurones were investigated. On P18, when dye coupling has virtually disappeared, application of 30 mM sodium propionate still reduced the amplitudes of EPSPs in all six neurones tested (by 61·8 ± 2·15%; Fig. 11*B*). Thus, the reduction in EPSP amplitude observed following intracellular acidification is probably due to direct interference of lowered pH or of organic acids with chemical synaptic transmission on either the pre- or postsynaptic site.

Effects of 1-octanol on input resistance and synaptic transmission

1-Octanol, one of the best characterized pharmacological agents known to reduce gap junctional conductance (Johnston, Simon & Ramon, 1980; Burt & Spray, 1988), applied at a concentration of 2 mM, increased input resistance in only four out of twelve neurones tested (by 47·33 ± 19·76%) between P2 and P9 (Fig. 12*A*). However, recordings were frequently less stable following 1-octanol application compared with recordings in the presence of organic acids. On P16–P18, when gap junction coupling has largely disappeared, 1-octanol had no significant effect on input resistance ($n = 4$; Fig. 12*E*).

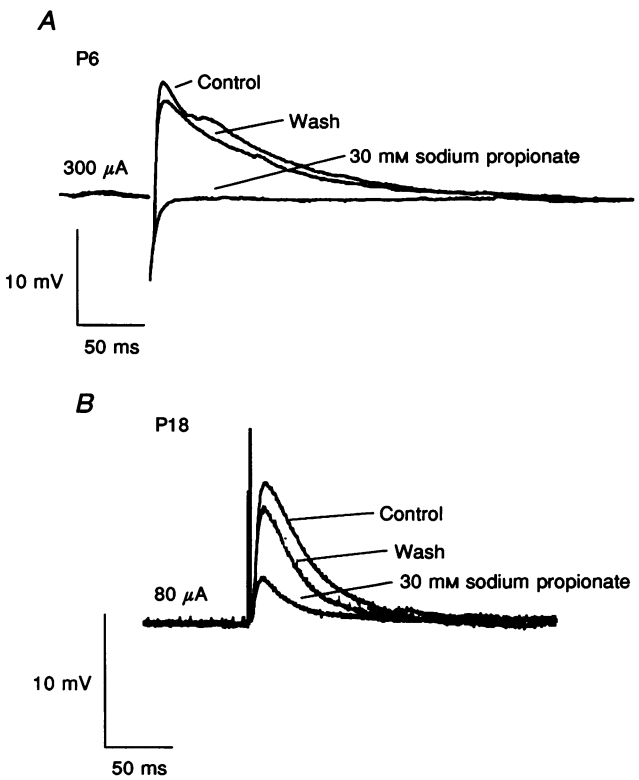

Figure 11. Effects of organic acids on excitatory synaptic potentials

A, in neurones recorded between P3 and P11, application of 30 mM sodium propionate reduced EPSP amplitudes by 20–100%. In the P6 neurone shown, the EPSP was completely suppressed. This inhibitory effect was reversible upon washout of sodium propionate (Wash). $V_m = -67$ mV. *B*, on P18, when gap junctions have disappeared, EPSPs were still severely reduced by acid application. $V_m = -70$ mV. NMDA and non-NMDA receptor-mediated components have not been separated in these experiments.

Between P2 and P9, 1-octanol decreased EPSP amplitudes in twelve out of fifteen neurones tested (by 64·96 ± 9·18%). In the remaining three cells, a 32–100% increase in EPSP size was observed (Fig. 12*B* and *C*). Between P16 and P18, 1-octanol still reduced EPSP amplitudes by 55·04 ± 2·57% ($n = 4$; Fig. 12*D*), indicating that 1-octanol also directly interferes with chemical synaptic transmission.

Effects of intracellular acidification on electrotonic potentials resembling EPSPs

Since weak organic acids as well as 1-octanol directly interfere with chemical synaptic transmission, we mimicked the amplitude and time course of EPSPs in order to study the effects of intracellular acidification on depolarizing electrotonic potentials. Transient depolarizing currents resembling glutamatergic postsynaptic currents as recorded from layer II–III neurones (Burgard & Hablitz, 1993) were injected, and the corresponding voltage responses measured (Fig. 13). In P4–P13 neurones, the amplitudes of these potentials ranged between 0·1 and 1·3 mV. To test for a possible activation of active conductances, we injected hyperpolarizing currents of equal amplitude and duration. In all five neurones tested, the voltage response to hyperpolarizing currents was absolutely symmetrical with the corresponding positive voltage deflection. The amplitudes

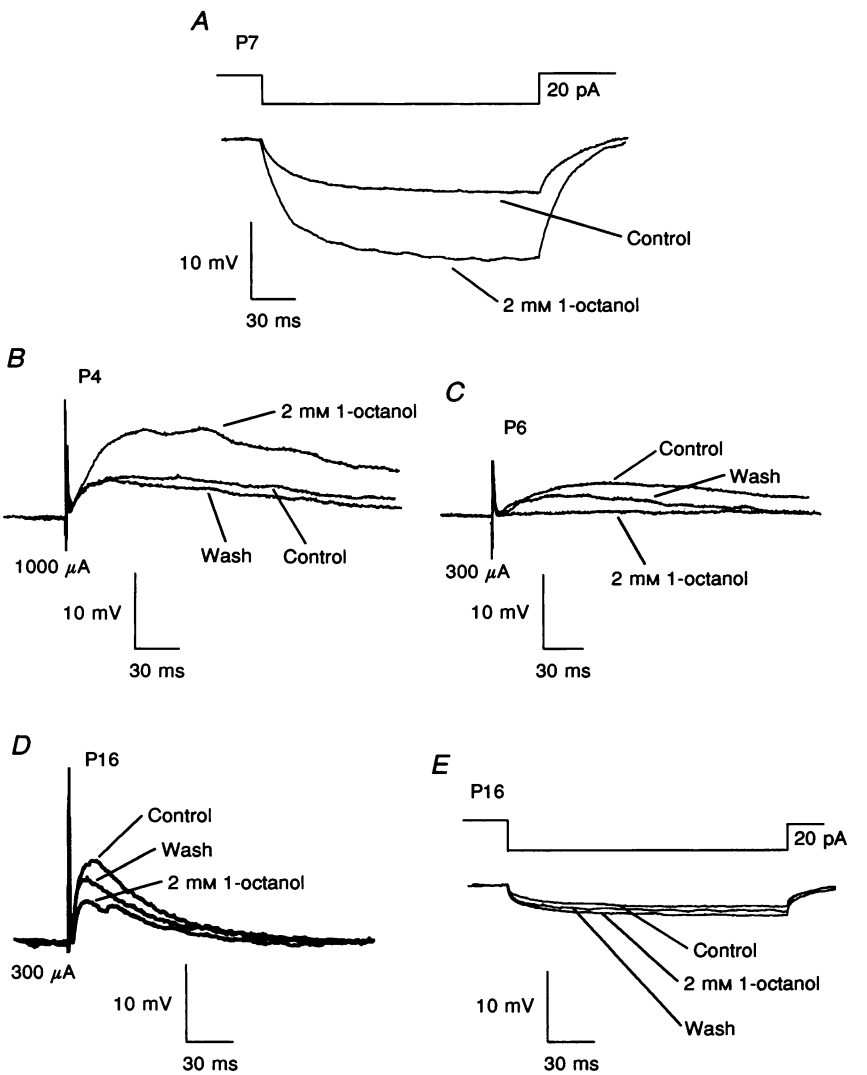

Figure 12. Effects of 1-octanol on input resistance and synaptic potentials

A, application of 2 mM 1-octanol increased input resistance in approximately one-third of the neurones tested. Recordings were made at resting membrane potential. *B*, in 3 out of 15 neurones, 1-octanol increased the EPSP amplitude. Stimulus strength, 1000 μA for 100 μs; $V_m = -62$ mV. *C*, in the majority of layer II–III neurones tested, 1-octanol suppressed excitatory synaptic transmission. Stimulus current strength, 300 μA for 100 μs; $V_m = -60$ mV. NMDA and non-NMDA receptor-mediated EPSP components have not been separated in these experiments. *D*, on P16, when gap junction coupling has strongly declined, 1-octanol also reduced EPSP amplitudes by approximately 50% (stimulus strength, 300 μA; $V_m = -76$ mV), whereas input resistance was not affected (*E*).

of these depolarizing electrotonic potentials significantly and reversibly increased following intracellular acidification (by 148·5 ± 49·6%; $n = 13$; Fig. 13*A–C*). The time course of these responses was found to be prolonged after lowering the intracellular pH in eight out of twelve neurones tested. The mean increase in the 10–90% rise time was 40·55 ± 14·15 ms; the mean increase in duration measured at half-maximal amplitude was 56·1 ± 28·6 ms. Voltage responses to simulated 'synaptic currents' were not affected by lowering intracellular pH in all neurones tested on P18 ($n = 8$; Fig. 13*D*), strongly suggesting that the effects observed in younger cells are due to changes in electrotonic membrane properties produced by gap junction closure.

DISCUSSION

In this study, we have presented evidence for the regulation of electrotonic communication between layer II–III pyramidal cells in neonatal rat frontal and sensorimotor cortex by changes in intracellular pH. Intracellular acidification caused a significant reduction in dye coupling, as well as an increase in input resistance and a reduction in electrotonic length. The results demonstrate that gap junctions affect electrotonic cell properties, suggesting that electrotonic coupling influences the efficacy of chemical synaptic transmission during the period of circuit formation. Furthermore, the developmental decline in variability of basic electrophysiological properties parallels the time course of uncoupling indicating that, apart from ion channel expression patterns and changes in membrane area, gap junctions might play a role in shaping the electrotonic structure of immature neocortical neurones.

Regulation of gap junction coupling by intracellular pH shifts

The present study complements previous findings that dye coupling between immature neocortical neurones is sensitive to shifts in intracellular pH. Thus, dye coupling between ventricular zone cells has been shown to decrease following intracellular acidification (Lo Turco & Kriegstein, 1991),

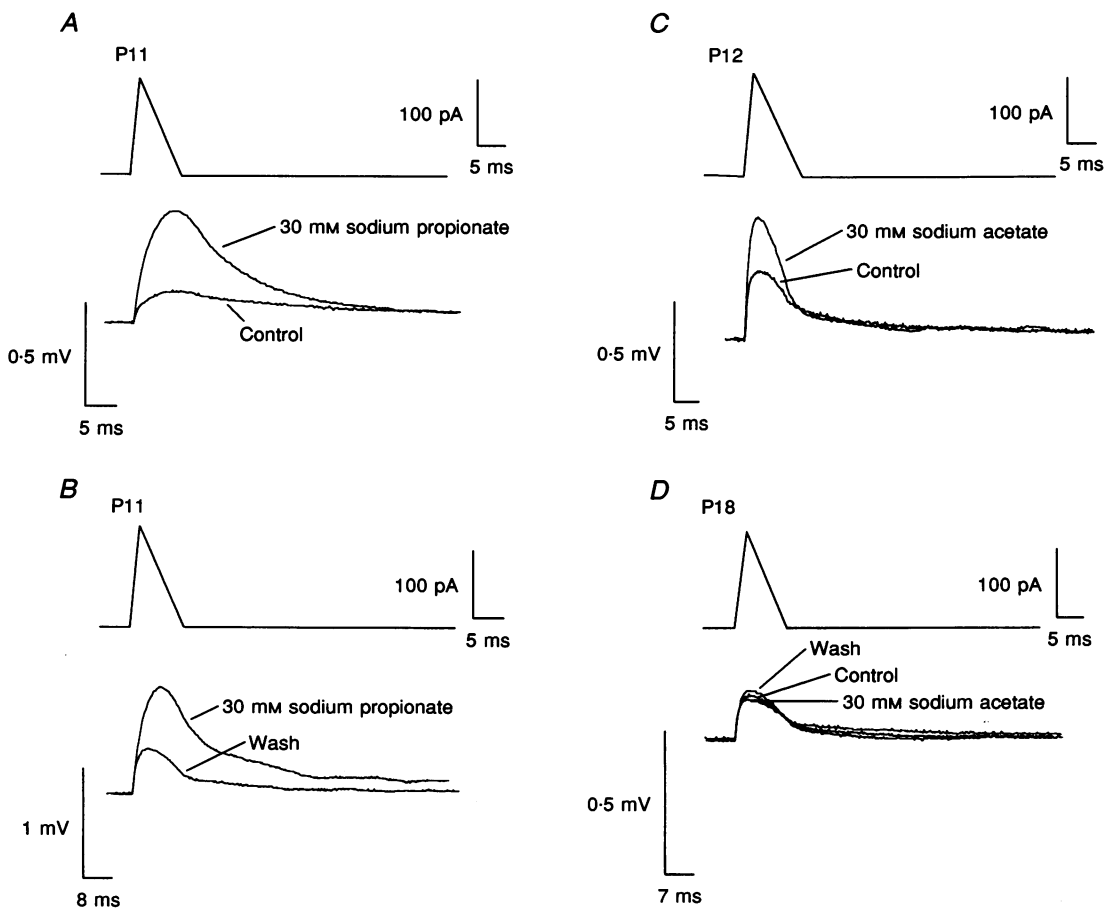

Figure 13. Effects of intracellular acidification on depolarizing electrotonic potentials induced by current injection

Depolarizing current pulses of 100 pA amplitude, 1 ms time to peak and 5 ms decay time were delivered via the patch pipette. *A* and *B*, application of 30 mM sodium propionate reversibly potentiated the 'artificial' EPSP. *C*, sodium acetate (30 mM) also enhanced voltage responses to short current stimuli. *D*, no significant effect of intracellular acidification was observed in neurones on P18. Recordings were made at resting membrane potential. All records are averages of 15 sweeps.

and equilibration of the external solution with 100% CO_2 caused an increase of more than 100% in the input resistance of these cells. Neuroblasts uncouple when migrating along radial glia (Lo Turco & Kriegstein, 1991) and gap junctions are newly formed when immature neurones reach their final position in the developing cortical plate. Electrotonic coupling between embryonic cortical plate cells is also sensitive to intracellular pH (Mienville *et al.* 1994). Saturation of the external solution with 100% CO_2 produced an increase in input resistance (61·5%) quantitatively similar to our results obtained with application of weak organic acids in postnatal neurones, suggesting that pH sensitivity of neocortical neurones does not change significantly after birth. 1-Octanol was also less effective in reducing junctional conductance in embryonic cortical plate cells (Mienville *et al.* 1994), as observed also in our study.

In the majority of our experiments, input resistance transiently decreased after washout of organic acids indicating that the transient intracellular alkalosis we measured following acidification increases gap junctional conductance. Although we did not attempt to quantify this result, our data suggest that, as previously reported in hippocampal neurones (Perez-Velaquez *et al.* 1994), electrotonic communication between neocortical neurones is modulated by intracellular acidification as well as alkalosis.

The technique of acidifying the cytoplasm using weak organic acids or CO_2 has been well characterized in isolated cell pairs where the junctional conductance and the cytoplasmic pH were measured simultaneously using pH-sensitive microelectrodes (Spray, Harris & Bennet, 1981). Intracellular acidification via membrane permeant organic acids allows the extracellular pH to be kept at physiological levels, whereas equilibration with 100% CO_2 causes extracellular acidification which might activate a proton-sensitive inward current (Krishtal & Pidoplichko, 1980). Replacement of one-fourth of the external NaCl by sodium propionate has been shown to decrease the internal pH by approximately 0·5 pH units in crayfish muscle (Sharp & Thomas, 1981); lactate and acetate lowered the internal pH by 0·39 and 0·57 pH units, respectively. In our preparation, optical recordings of intracellular pH revealed an acidic shift of approximately 0·4–0·5 pH units following application of 30 mM sodium propionate. A pH shift from 7·7 to 6·6 is necessary to cause complete uncoupling in amphibian blastomeres (Spray *et al.* 1981). However, such direct correlations between changes in cytoplasmic pH and electrophysiologically determined gap junctional conductance are not yet available for mammalian central neurones in intact tissue. A significant reduction in dye coupling after incubation in propionate has been reported for CA3 pyramidal neurones (MacVicar & Jahnsen, 1985) and application of propionate to achieve intracellular acidification has been used recently by Perez-Velaquez *et al.* (1994) to suppress gap junction coupling between CA1 neurones in rat hippocampus. Although dye coupling, fast prepotential (FPP) frequency, as well as the spread of epileptiform field bursts were reduced by this treatment, no effect on input resistance was observed. This is probably due to a smaller number of coupled neurones in the hippocampus of P20–P30 rats compared with the immature neocortex. The maximum number of coupled cells observed by those authors was two under control conditions, and three to five in calcium-free medium using Lucifer Yellow (LY) as a tracer, whereas LY stained up to eight coupled neurones in the neocortex at P7–P8 (Peinado *et al.* 1993). LY-detected dye coupling between guinea-pig pyramidal cells on P6 has been reported to be rather insensitive to changes in intracellular pH (Connors, Benardo & Prince, 1984). However, LY does not represent an optimal tracer to study dye coupling between postnatal neocortical neurones since gap junction permeability of this molecule is low (Peinado *et al.* 1993).

To exclude non-specific effects of propionate, we have additionally used two different weak organic acids to lower intracellular pH. Both sodium acetate and sodium lactate produced effects on dye coupling and passive membrane properties similar to those of sodium propionate. Sodium acetate has recently been reported to uncouple taste receptor cells in a slice preparation of *Necturus* lingual epithelium (Bigiani & Roper, 1994), leading to an increase in input resistance and a decrease in membrane capacitance.

The subunits of gap junctions, i.e. the connexins, differ in their pH sensitivity. Connexin 43 has been demonstrated to be more sensitive to intracellular acidification than connexin 32 (Liu, Taffet, Stoner, Delmar, Vallano & Jalife, 1993). So far, the connexin composition of gap junctions formed between neocortical neurones has not been elucidated. The effects on electrotonic membrane properties that we observed were in the 50% range, but displayed considerable variability, ranging between 20 and 300%. Apart from differences in connexin composition of gap junctions, this variability might be due to the variability of gap junction conductance, intercellular differences in location of coupling sites or to different degrees of buffering as a consequence of dialysis with the pipette solution. The electrophysiologically detectable effect should further depend on the number of gap junctions per coupled neurone as well as the subcellular location of the junctions. In the developing neocortex, the majority of gap junctions have been shown to occur at dendrodendritic and dendrosomatic sites (Peinado *et al.* 1993). Our results confirm these observations, although some injections resulted in two or three darkly stained and closely apposed somata, suggesting somatosomatic coupling sites. Electron microscopic data also suggest contact sites between apical dendrites (Parnavelas & Nadarajah, 1994). Single channel conductances and gating properties of neocortical gap junctions

have not been characterized so far, but even if only small currents flow through individual junctions, the large number of neurones coupled together suggests marked influences on the apparent electrotonic structure of an individual neurone.

Influence of gap junction coupling on electrophysiological properties

We have used the patch clamp technique to study changes in electrotonic properties after uncoupling since the high seal resistance allows a more accurate measurement of passive membrane properties than microelectrode recordings. Compared with patch clamp recordings, the apparent input resistance of hippocampal neurones has been shown to decrease by a factor of two to four, due to the leak produced by penetration with sharp microelectrodes (Spruston, Jaffe, Williams & Johnston, 1993).

The electrophysiological consequences of gap junction coupling are twofold. First, the apparent increase in membrane area influences electrotonic parameters, and second, electrical signals such as synaptic potentials or action potentials generated in neighbouring neurones might be directly transmitted via these cytoplasmic contacts. Uncoupling of a single neurone from the syncytial cluster is expected to increase its apparent input resistance, which depends on specific membrane resistance and cell geometry, and to reduce its effective membrane capacitance and electrotonic length. We have observed both an increase in input resistance, and a decrease in electrotonic length following intracellular acidification. Thus, a synaptic current of a given amplitude should produce a larger synaptic potential which is less attenuated during propagation towards the cell soma, resulting in increased excitability. The effect of acidification on the membrane time constant (τ_0) was heterogenous. The time constant is determined by both membrane resistance and membrane capacitance. In the majority of neurones tested, the membrane time constant decreased, which might be explained by a decrease in membrane capacitance. In some cells, the membrane time constant was found to be prolonged after gap junction closure, suggesting that the increase in membrane resistance was more prominent in these cases. However, a clear resolution of this problem requires simultaneous and direct determination of input resistance and membrane capacitance. Changes in the membrane time constant might have significant consequences for signal processing since temporal summation of synaptic potentials is affected.

The most prominent example of electrotonic consequences of extensive gap junction coupling is found in the vertebrate retina. The strong coupling between horizontal and amacrine cells prevents the measurement of input resistance (Miyachi, Kato & Nakaki, 1994). In these neurones, signal transfer via gap junctions plays an important role in shaping receptive fields. A correlation of low input resistance with a high degree of electrical coupling has also been shown in rat ventricular zone cells (Lo Turco & Kriegstein, 1991). Although we observed an increase in input resistance after uncoupling via intracellular acidification in an acute experiment, input resistance declined significantly during postnatal development, despite progressive developmental uncoupling of pyramidal neurones. This apparent contradiction might be explained by an increase in membrane surface area due to dendritic branching and increasing soma size outweighing the decrease in surface area caused by uncoupling. Apart from this, increasing ion channel densities (Courand *et al.* 1886), as well as higher frequencies of spontaneous synaptic currents (Burgard & Hablitz, 1993) cause the specific membrane resistance to decrease, leading to a further reduction in apparent input resistance. The membrane time constant also declined during postnatal development, which might be due primarily to decreasing membrane resistance. However, an additional effect of decreasing cell capacitance after uncoupling cannot be excluded. Similar developmental changes in passive membrane properties have been reported in layer V pyramidal neurones (McCormick & Prince, 1987; Kasper *et al.* 1994). We additionally analysed the developmental changes in the first equalizing time constant (Rall, 1969) and the electrotonic length. Both parameters declined significantly with increasing postnatal age suggesting that, despite on-going morphological differentiation, neurones become electrotonically more compact. This effect can only be explained by a significant influence of uncoupling on electrotonic structure. Since coupling sites are predominantly located in the dendritic tree, the decrease in the first equalizing time constant, which reflects charging of the dendrites (Rall, 1969), might indicate a reduction in the functional extent of the dendritic tree upon disappearance of gap junctions. Thus, from the development of electrotonic properties, synaptic potentials are expected to become faster and less attenuated during postnatal development. Since a significant decline in EPSP duration has been shown to be caused by a diminishing contribution of NMDA receptor-mediated components (Burgard & Hablitz, 1993), we isolated the non-NMDA receptor-mediated component to study the influence of changes in electrotonic structure on synaptic signals.

The duration of non-NMDA receptor-mediated EPSPs measured at half-maximal amplitude decreased by approximately 50% with development from P1–P2 to P18. The decrease in EPSP duration cannot be attributed exclusively to the shortening of membrane time constants since its developmental change was still significant after normalization of the EPSP duration with respect to the membrane time constant. A reduction in EPSP duration has also been reported for compound EPSPs in neocortical layer V neurones (Kasper *et al.* 1994). In our experiments, EPSP rise times did not change significantly during

postnatal development of layer II–III neurones. In contrast, Kasper *et al.* (1994) observed a decline in compound EPSP rise times in layer V pyramidal cells. The developmental changes in the duration of non-NMDA receptor-mediated EPSPs can be explained by simultaneous alterations in electrotonic cell properties induced by the disappearance of gap junctions. However, a developmental switch in non-NMDA receptor subunit composition, which might affect EPSP kinetics, cannot be excluded. Indeed, such developmental changes in non-NMDA receptor subunit expression during maturation of the rat neocortex have been described by *in situ* hybridization studies (Pellegrini-Giampietro, Bennett & Zukin, 1992). In conclusion, a number of developmental changes in electrophysiological properties point to a contribution of gap junction coupling to the shaping of the electrotonic features of an immature pyramidal neurone. However, concomitant developmental alterations in ion channel expression, as well as progressive morphological differentiaton, preclude a direct correlation.

Depolarizations spreading through gap junctions have been demonstrated to facilitate spike generation in crayfish mechanoreceptor afferents (El Manira, Cattaert, Wallen, Dicaprio & Clarac, 1993). Action potentials invading the recorded neurone from its coupled neighbours have been recorded as FPPs or short-latency depolarizations (SLDs) in rat hippocampus (Taylor & Dudek, 1982), rat nucleus accumbens (O'Donnell & Grace, 1993), and in the developing rat neocortex (Connors *et al.* 1983). The notion of FPPs being coupling potentials has been verified by MacVicar & Dudek (1981) by means of pair recordings in rat hippocampal slices. The propagation of synaptic signals via gap junctions has been suggested by Perez-Velaquez *et al.* (1994). These authors abolished epileptiform field potential activity by the application of gap junction blockers. However, our data show that both 1-octanol, as well as sodium propionate, inhibit excitatory synaptic transmission even during developmental stages when gap junction coupling has virtually disappeared. In order to investigate the probable effects of a gap junction block on fast rising depolarizing electrotonic potentials, we mimicked excitatory synaptic potentials by injecting transient currents resembling glutamatergic EPSCs as recorded from layer II–III neurones. The resulting voltage responses were similar to small EPSPs with amplitudes ranging between 0·1 and 1·3 mV. Due to the frequency dependence of voltage attenuation (Spruston *et al.* 1993), these artificial synaptic potentials were more strongly potentiated following gap junction closure via intracellular acidification than voltage responses to hyperpolarizing square-wave current pulses. Although the current injection sites were somatic, thus differing from the predominantly dendritic location of the real excitatory input to neocortical pyramidal cells (Miller, 1988), we conclude that the changes in electrotonic cell properties brought about by gap junction closure might dramatically enhance the efficacy of fast synaptic inputs.

Functional significance of the pH-dependent regulation of gap junction coupling in the neocortex

The pH sensitivity of gap junctions might be significant for the function of immature neocortical neurones. Intracellular pH changes occur during synchronized neuronal activity, especially during epileptiform activity (Chesler & Kaila, 1992). Compared with the adult rat neocortex, an enhanced vulnerability of the immature neocortex to convulsant drugs, especially during the second and third postnatal week, has been reported (Hablitz, 1987). Amplitudes of epileptiform activity and the degree of its synchronization are more pronounced during this developmental period and the activity can be generated by multiple foci (Sutor, Hablitz, Rucker & ten Bruggencate, 1994). These observations might be explained, at least in part, by a facilitated spread of excitatory currents through gap junctions. On the other hand, very extensive electrical coupling of neurones via gap junctions, as observed during the first postnatal week, apparently decreases the input resistance of the neurones thereby counteracting the ability of the cells to generate large potential changes. This shunting effect might be the cause of the virtual absence of evoked epileptiform activity observed *in vitro* during the first week of postnatal development of the rat neocortex (Sutor *et al.* 1994).

However, electrotonic communication between neurones does not only affect the behaviour of immature neocortical neuronal circuits during pathophysiological conditions, but also certainly influences synaptogenesis within the neocortex. The efficacy of an excitatory synaptic input to a given neurone is partly determined by the electrotonic properties of the postsynaptic cell. Since we have shown that a block of gap junctions results in changes in these properties, it is legitimate to assume that gap junctions might have a crucial function during selective stabilization and potentiation of chemical synapses and may thus play an important role in shaping cortical circuitries.

Beyer, E. C. (1993). Gap junctions. *International Review of Cytology* **137C**, 1–37.

Bigiani, A. & Roper, S. D. (1994). Reduction of electrical coupling between *Necturus* taste receptor cells, a possible role in acid taste. *Neuroscience Letters* **176**, 212–216.

Blanton, M. G., Lo Turco, J. J. & Kriegstein, A. R. (1989). Whole cell recordings from neurons in slices of reptilian and mammalian cerebral cortex. *Journal of Neuroscience Methods* **30**, 203–210.

Buckler, K. J. & Vaughan-Jones, R. D. (1990). Application of a new pH-sensitive fluoroprobe (carboxy-SNARF-1) for intracellular pH measurement in small, isolated cells. *Pflügers Archiv* **417**, 234–239.

Burgard, E. C. & Hablitz, J. J. (1993). Developmental changes in NMDA and non-NMDA receptor-mediated synaptic potentials in rat neocortex. *Journal of Neurophysiology* **69**, 230–240.

BURT, J. M. & SPRAY, D. C. (1988). Single channel events and gating behaviour of the cardiac gap junction channel. *Proceedings of the National Academy of Sciences of the USA* **85**, 3431–3434.

CEPEDA, J., WALSH, J. P., PEACOCK, W., BUCHWALD, N. A. & LEVINE, M. S. (1993). Dye-coupling in human neocortical tissue resected from children with intractable epilepsy. *Cerebral Cortex* **3**, 95–107.

CHESLER, M. & KAILA, K. (1992). Modulation of pH by neuronal activity. *Trends in Neurosciences* **15**, 396–402.

CONNORS, B. W., BENARDO, L. S. & PRINCE, D. A. (1983). Coupling between neurons of the developing rat neocortex. *Journal of Neuroscience* **3**, 773–782.

CONNORS, B. W., BENARDO, L. S. & PRINCE, D. A. (1984). Carbon dioxide sensitivity of dye coupling among glia and neurons of the neocortex. *Journal of Neuroscience* **4**, 1324–1330.

CONNORS, B. W. & GUTNICK, M. J. (1990). Intrinsic firing patterns of diverse neocortical neurons. *Trends in Neurosciences* **13**, 99–104.

COURAND, F., MARTIN-MOUTOT, N., KOULAKOFF, A. & BERWALD-NEFFER, Y. (1986). Neurotoxin sensitive sodium channels in neurons developing in vivo and in vitro. *Journal of Neuroscience* **3**, 192–198.

EL MANIRA, A., CATTAERT, D., WALLEN, P., DICAPRIO, R. A. & CLARAC, F. (1993). Electrical coupling of mechanoreceptor afferents in the crayfish: A possible mechanism for enhancement of sensory signal transmission. *Journal of Neurophysiology* **69**, 2248–2251.

HABLITZ, J. J. (1987). Spontaneous ictal-like discharges and sustained potential shifts in the developing rat neocortex. *Journal of Neurophysiology* **58**, 1052–1065.

JOHNSTON, M. F., SIMON, S. A. & RAMON, F. (1980). Interaction of anaesthetics with electrical synapses. *Nature* **286**, 498–500.

KANDLER, K., DOUGLAS, S. B. & KATZ, L. C. (1994). Neuronal dye-coupling and spontaneous activity are inversely related in developing ferret visual cortex. *Society for Neuroscience Abstracts* **20**, 215.

KASPER, E. M., LARKMAN, A. U., LÜBKE, J. & BLAKEMORE, C. (1994). Pyramidal neurons in layer 5 of the rat visual cortex. II. Development of electrophysiological properties. *Journal of Comparative Neurology* **399**, 475–494.

KRISHTAL, O. A. & PIDOPLICHKO, V. I. (1980). A receptor for protons in the nerve cell membrane. *Neuroscience* **5**, 2325–2327.

LIU, S., TAFFET, S., STONER, L., DELMAR, M., VALLANO, M. L. & JALIFE, J. (1993). A structural basis for the unequal sensitivity of the major cardiac and liver gap junctions to intracellular acidification: The carboxyl tail length. *Biophysical Journal* **64**, 1422–1433.

LO TURCO, J. J. & KRIEGSTEIN, A. R. (1991). Clusters of coupled neuroblasts in embryonic neocortex. *Science* **252**, 563–566.

MCCORMICK, D. A. & PRINCE, D. A. (1987). Post-natal development of electrophysiological properties of rat cerebral cortical pyramidal neurones. *Journal of Physiology* **393**, 743–762.

MACVICAR, B. A. & DUDEK, F. E. (1981). Electrotonic coupling between pyramidal cells: A direct demonstration in rat hippocampal slices. *Science* **213**, 782–785.

MACVICAR, B. A. & JAHNSEN, H. (1985). Uncoupling of CA3 pyramidal neurons by propionate. *Brain Research* **330**, 141–145.

MIENVILLE, J. M., LANGE, G. D. & BARKER, J. L. (1994). Reciprocal expression of cell–cell coupling and voltage-dependent Na current during embryogenesis of rat telencephalon. *Developmental Brain Research* **77**, 89–95.

MILLER, M. (1988). Development of projection and local circuit neurons in neocortex. In *Cerebral Cortex*, vol. VII, ed. PETERS, A. & JONES, E. G., pp. 133–175. Plenum Press, New York.

MIYACHI, E.-I., KATO, C. & NAKAKI, T. (1994). Arachidonic acid blocks gap junctions between retinal horizontal cells. *NeuroReport* **5**, 485–488.

O'DONNELL, P. & GRACE, A. A. (1993). Dopaminergic modulation of dye coupling between neurons in the core and shell regions of the nucleus accumbens. *Journal of Neuroscience* **13**, 3456–3471.

PARNAVELAS, J. G. & NADARAJAH, B. (1994). Gap junctions are prevalent in the developing cerebral cortex. *Society for Neuroscience Abstracts* **20**, 1672.

PAYSAN, J., BOLZ, J., MOHLER, H. & FRITSCHY, J.-M. (1994). $GABA_A$ receptor $\alpha 1$ subunit, an early marker for area specification in developing rat cerebral cortex. *Journal of Comparative Neurology* **350**, 133–149.

PEINADO, A., YUSTE, R. & KATZ, L. C. (1993). Extensive dye coupling between rat neocortical neurons during the period of circuit formation. *Neuron* **10**, 103–114.

PELLEGRINI-GIAMPIETRO, D. E., BENNETT, M. V. & ZUKIN, R. S. (1992). Are Ca^{2+}-permeable kainate/AMPA receptors more abundant in immature brain? *Neuroscience Letters* **144**, 65–69.

PEREZ-VELAQUEZ, J. L., VALIANTE, T. A. & CARLEN, P. L. (1994). Modulation of gap junctional mechanisms during calcium-free induced field burst activity: A possible role for electrotonic coupling in epileptogenesis. *Journal of Neuroscience* **14**, 4308–4317.

PERKINS, A. T. & TEYLER, T. J. (1988). A critical period for long-term potentiation in the developing rat visual cortex. *Brain Research* **439**, 222–229.

RALL, W. (1969). Time constant and electrotonic length of membrane cylinders and neurons. *Biophysical Journal* **9**, 1483–1508.

SHARP, A. P. & THOMAS, R. C. (1981). The effects of chloride substitution on intracellular pH in crab muscle. *Journal of Physiology* **312**, 71–80.

SPRAY, D. C., HARRIS, A. L. & BENNET, M. V. L. (1981). Gap junctional conductance is a simple and sensitive function of intracellular pH. *Science* **211**, 712–715.

SPRUSTON, N., JAFFE, D. B., WILLIAMS, S. H. & JOHNSTON, D. (1993). Voltage- and space-clamp errors associated with the measurement of electrotonically remote synaptic events. *Journal of Neurophysiology* **70**, 781–802.

SUTOR, B., HABLITZ, J. J., RUCKER, F. & TEN BRUGGENCATE, G. (1994). Spread of epileptiform activity in the immature rat neocortex studied with voltage-sensitive dyes and laser scanning microscopy. *Journal of Neurophysiology* **72**, 1756–1768.

TAYLOR, C. P. & DUDEK, F. E. (1982). A physiological test for electrotonic coupling between CA1 pyramidal cells in rat hippocampal slices. *Brain Research* **235**, 351–357.

YUSTE, R., PEINADO, A. & KATZ, L. C. (1992). A system of neuronal domains in developing neocortex. *Science* **257**, 665–668.

Acknowledgements

The authors would like to thank J. Wächtler and P. Grafe for introducing us to the technique of optical monitoring of intracellular pH, K. Feasey-Truger and G. ten Bruggencate for reading the manuscript and helpful discussions, L. Kargl for excellent technical assistance and Dr Olpe (Ciba-Geigy, Basel, Switzerland) for the supply of CGP 35348. The work was supported by the Deutsche Forschungsgemeinschaft (SFB 220/A9).

Received 24 March 1995; accepted 7 July 1995.